



# New Ru<sub>3</sub>(CO)<sub>12</sub> derivatives with bulky diphosphine ligands: synthesis, structure and catalytic potential for olefin hydroformylation

Enrique Lozano Diz, Antonia Neels, Helen Stoeckli-Evans, Georg Süss-Fink \*

*Institut de Chimie, Université de Neuchâtel, Case postale 2, CH-2007 Neuchâtel, Switzerland*

Received 22 March 2001; accepted 17 May 2001

## Abstract

The diphosphine clusters Ru<sub>3</sub>(CO)<sub>10</sub>(dcpm) (**1**) and Ru<sub>3</sub>(CO)<sub>10</sub>(F-dppe) (**2**) as well as the bis(diphosphine) clusters Ru<sub>3</sub>(CO)<sub>8</sub>(dcpm)<sub>2</sub> (**3**) and Ru<sub>3</sub>(CO)<sub>8</sub>(F-dppe)<sub>2</sub> (**4**) have been synthesised from Ru<sub>3</sub>(CO)<sub>12</sub> and the bulky diphosphines 1,2-bis[bis(pentafluorophenyl)phosphino]ethane (F-dppe) and bis(dicyclohexylphosphino)methane (dcpm). While the single-crystal X-ray structure analyses of **1**, **2** and **3** show the expected μ<sub>2</sub>-η<sup>2</sup> coordination of the diphosphine ligands, that of **4** reveals an unusual structure with one μ<sub>2</sub>-η<sup>2</sup>-diphosphine and one μ<sub>1</sub>-η<sup>2</sup>-diphosphine ligand. The clusters **1–4** catalyse the hydroformylation of ethylene and propylene to give the corresponding aldehydes, **2** showing higher activities than those observed for Ru<sub>3</sub>(CO)<sub>12</sub> and Ru<sub>3</sub>(CO)<sub>10</sub>(dppe). © 2001 Elsevier Science Ltd. All rights reserved.

*Keywords:* Ruthenium; Carbonyl; Clusters; Diphosphine; Hydroformylation

## 1. Introduction

The chemistry of dodecacarbonyltriruthenium with diphosphines has been extensively studied; numerous Ru<sub>3</sub>(CO)<sub>12</sub> derivatives containing one, two or three diphosphine ligands have been synthesised and fully characterised [1]. The structures of many derivatives have been reported over the last two decades: Ru<sub>3</sub>(CO)<sub>10</sub>(dppm) (dppm = bis(diphenylphosphino)methane) [2], Ru<sub>3</sub>(CO)<sub>8</sub>(dppm)<sub>2</sub> [3], Ru<sub>3</sub>(CO)<sub>6</sub>(dppm)<sub>3</sub> [4], Ru<sub>3</sub>(CO)<sub>10</sub>(dppe) (dppe = bis(diphenylphosphino)ethane) [5], Ru<sub>3</sub>(CO)<sub>8</sub>(dppe)<sub>2</sub> [5].

The catalytic potential of these derivatives has been intermittently studied, mainly for the hydrogenation of terminal olefins; only Ru<sub>3</sub>(CO)<sub>10</sub>(dppm) and Ru<sub>3</sub>(CO)<sub>8</sub>(dppm)<sub>2</sub> have been tested more widely as catalysts for hydrogenation (1-hexene, 1-hexyne, styrene, cyclohexene, benzene, acetone, cyclohexanone, acrolein, crotonaldehyde, cinnamaldehyde, acetonitrile, benzophenone, nitrobenzene), isomerisation reactions (1-hexene, 1-

hexyne, 1-methylcyclohexene, allylic alcohol), hydroformylation reactions (1-hexene) and for amination reactions (alcohols, olefins) [6,7]. Other ruthenium clusters containing diphosphine ligands such as H<sub>4</sub>Ru<sub>4</sub>(CO)<sub>10</sub>(dppm), H<sub>2</sub>Ru<sub>3</sub>(E)(CO)<sub>5</sub>(dppm)<sub>2</sub> (E = O, S), have been tested as catalysts for the hydrogenation of cyclohexene [8,9].

On the other hand, bulky phosphine ligands are known to allow unusual structures and unsaturated configurations for steric reasons [10–13]. We therefore decided to study the chemistry of Ru<sub>3</sub>(CO)<sub>12</sub> with the bulky diphosphine ligands bis(perfluoro-diphenylphosphino)ethane (F-dppe) and bis(dicyclohexylphosphino)methane (dcpm), in order to see if the sterically crowded pentafluorophenyl or cyclohexyl substituents impose new structural features on the trinuclear complexes formed, and what effect these substituents have on the catalytic properties of the complexes.

In this paper, we report the synthesis, molecular structure and catalytic hydroformylation properties of the new diphosphine clusters Ru<sub>3</sub>(CO)<sub>10</sub>(dcpm) (**1**) and Ru<sub>3</sub>(CO)<sub>10</sub>(F-dppe) (**2**) and also that of the bis(diphosphine) clusters Ru<sub>3</sub>(CO)<sub>8</sub>(dcpm)<sub>2</sub> (**3**) and Ru<sub>3</sub>(CO)<sub>8</sub>(F-dppe)<sub>2</sub> (**4**). Cluster **4** indeed turns out to have an

\* Corresponding author. Tel.: +41-32-718-2406; fax: +41-32-718-2511.

*E-mail address:* georg.suess-fink@unine.ch (G. Süss-Fink).

Table 1  
IR and NMR data of clusters 1–4

	$\nu(\text{CO})$ ( $\text{cm}^{-1}$ ) <sup>a</sup>	$\delta(^1\text{H})$ (ppm) <sup>b</sup>	$\delta(^{31}\text{P}\{^1\text{H}\})$ (ppm) <sup>b</sup>	$\delta(^{19}\text{F})$ (ppm) <sup>b</sup>
1	2078 m, 2013 m, 2001 vs, 1964 w 1951 m, 1943 m	2.06–1.23 (m)	27.5 (s)	
2	2092 s, 2049 w, 2029 vs, 1984 m, 1961 m	2.66 (d, $J_{\text{PH}} = 32.2$ Hz)	16.2 (s)	–129.9 (8 $F_o$ ), –145.6 (4 $F_p$ ), –157.7 (8 $F_m$ )
3	2028 m, 2004 w, 1989 w, 1957 s, 1950 s, 1932 m, 1870m	2.65–1.85 (m)	32.3 (d, $J_{\text{PP}} = 34.5$ Hz), 28.8 (d, $J_{\text{PP}} = 34.5$ Hz)	
4	2060 w, 2050 (sh), 2044 (sh), 2012 s, 2002 (sh), 1984 vs, 1934 m, 1871 w	2.71–2.46 (m)	35.6 (dt, $J_{\text{PP}} = 106.2$ ; $J_{\text{PP}} = 77.2$ ), 16.5 (dt, $J_{\text{PP}} = 106.2$ ; $J_{\text{PP}} = 77.2$ )	–122.0 (8 $F_o$ ), –129.8 (4 $F_o$ ), –146.4 (4 $F_p$ ), –148.0 (4 $F_p$ ), –158.3 (8 $F_m$ ), –159.1 (8 $F_m$ )

<sup>a</sup> In cyclohexane.

<sup>b</sup> In  $\text{CDCl}_3$ .

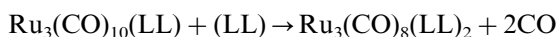
unusual structure containing one F-dppe ligand in a conventional  $\mu_2$ - $\eta^2$  coordination mode and the second F-dppe ligand in an unconventional  $\mu_1$ - $\eta^2$  coordination mode.

## 2. Results and discussion

The thermal reaction of  $\text{Ru}_3(\text{CO})_{12}$  with the diphosphine dcpm or F-dppe in refluxing tetrahydrofuran (thf) leads, depending on the ratio of the reactants, to the corresponding diphosphine clusters  $\text{Ru}_3(\text{CO})_{10}$ - (dcpm) (**1**) and  $\text{Ru}_3(\text{CO})_{10}$ (F-dppe) (**2**), respectively, as well as to the bis(diphenylphosphine) clusters  $\text{Ru}_3(\text{CO})_8$ (dcpm)<sub>2</sub> (**3**) and  $\text{Ru}_3(\text{CO})_8$ (F-dppe)<sub>2</sub> (**4**). Equimolar amounts of  $\text{Ru}_3(\text{CO})_{12}$  and the diphosphine produce mainly the diphosphine derivatives. The four compounds, which can be isolated by preparative thin-layer chromatography, form air-stable, red (**1**, **2**) or orange (**3**, **4**) crystalline solids.



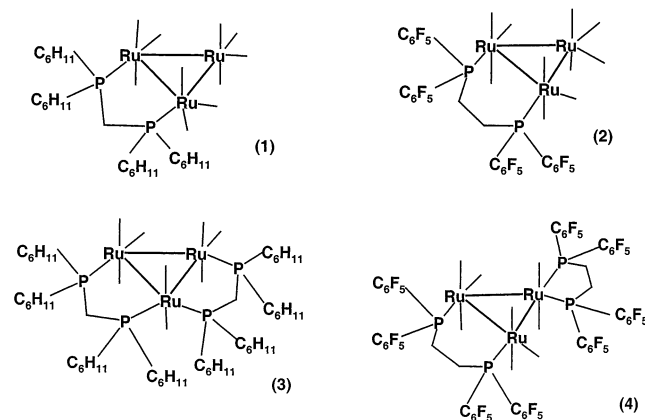
1: LL = dcpm, 2: LL = F-dppe



3: LL = dcpm, 4: LL = F-dppe

In the infrared spectra (Table 1), both **1** and **2** display a  $\nu(\text{CO})$  pattern characteristic for  $\text{Ru}_3(\text{CO})_{10}$ - (LL) clusters, which compares well with that observed for  $\text{Ru}_3(\text{CO})_{10}(\text{dppe})$  [5] and  $\text{Ru}_3(\text{CO})_{10}(\text{dppm})$  [14]. The  $^1\text{H}$  NMR spectra show the expected signals for the F-dppe and the dcpm ligands, while in the  $^{31}\text{P}\{^1\text{H}\}$  NMR spectra, **1** and **2** give rise to only one signal for the two equivalent phosphorus atoms (Table 1). The  $^{31}\text{P}$  resonance of **1** shows a shift ( $\delta = 27.5$  ppm) which compares well with those of the analogous cluster  $\text{Ru}_3(\text{CO})_{10}(\text{dppm})$  ( $\delta = 20.6$  ppm) [3], while the  $^{31}\text{P}$  signal of **2** is less deshielded ( $\delta = 16.2$  ppm) than that of the  $\text{Ru}_3(\text{CO})_{10}(\text{dppe})$  analogue ( $\delta = 41.16$  ppm), due to the presence of the fluorine (Scheme 1).

The molecular structures of the two  $\text{Ru}_3(\text{CO})_{10}(\text{LL})$  clusters have been determined by X-ray analysis of single crystals of **1** and **2** obtained by crystallisation from dichloromethane. For **1**, four independent molecules per asymmetric unit were found. The com-



Scheme 1.

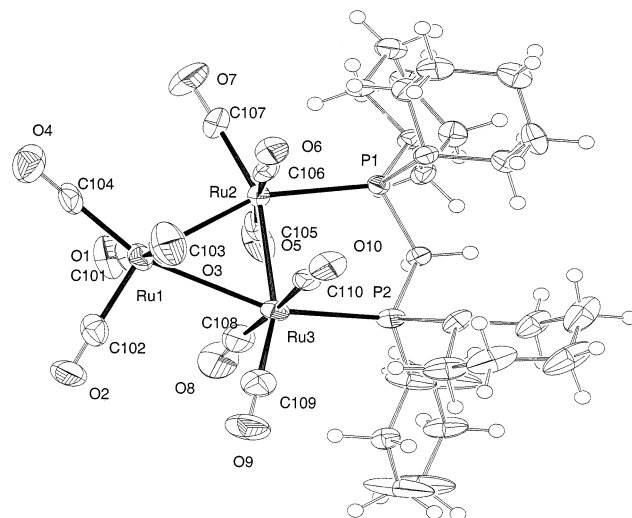
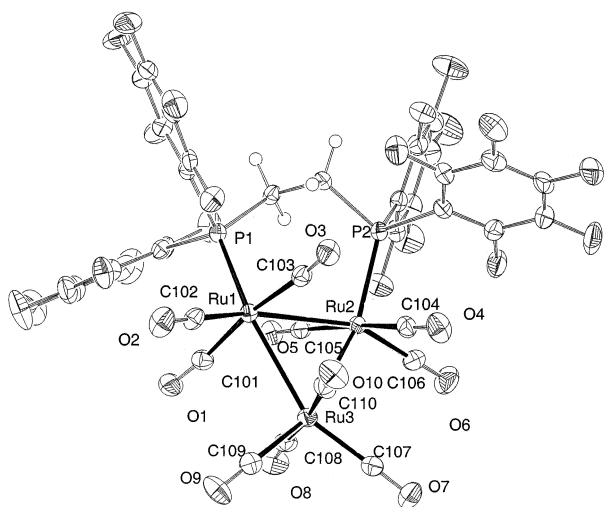


Fig. 1. ORTEP representation of **1** (molecule 1).

Fig. 2. ORTEP representation of **2**.

compounds **1** and **2** are depicted in Fig. 1 (molecule **1**) and Fig. 2, respectively. Important bond lengths and angles are presented in Table 2 and Table 3. Both clusters contain a closed triruthenium skeleton with an almost isosceles  $\text{Ru}_3$  triangle. The Ru–Ru distances (**1**: 2.8378(7), 2.8384(7), 2.8596(8) Å; **2**: 2.8422(4), 2.8494(4), 2.8684(4) Å) agree well with those observed in  $\text{Ru}_3(\text{CO})_{10}(\text{dppm})$  (2.834(1), 2.841(1), 2.860(1) Å) [2] and in  $\text{Ru}_3(\text{CO})_{10}(\text{dppe})$  (2.847(1), 2.856(1), 2.855(1) Å) [5]. As expected, the diphosphine ligands are equatori-

ally coordinated in **1** and **2**, the two phosphorus atoms being slightly out of the  $\text{Ru}_3$  plane (twist effect), one above and one below (torsion angles in **1**: P(1)–Ru(2)–Ru(3)–P(2) 11.39(6)°; torsion angles in **2**: P(1)–Ru(1)–Ru(2)–P(2) 31.94(3)°; distances of the phosphorus atoms from the  $\text{Ru}_3$ -plane: P(1): 0.6936 Å and P(2): –0.5685 Å).

With an excess of dcpm or F-dppe, the thermal reaction of  $\text{Ru}_3(\text{CO})_{12}$  gives mainly the corresponding bis(diphenylphosphine) clusters  $\text{Ru}_3(\text{CO})_8(\text{dcpm})_2$  (**3**) and  $\text{Ru}_3(\text{CO})_8(\text{F-dppe})_2$  (**4**), isolated by preparative thin-layer chromatography.

The IR spectra of compounds **3** and **4** show very different  $\nu(\text{CO})$  absorption patterns (Table 1), suggesting different structural features. As the  $\nu(\text{CO})$  pattern of **3** is analogous to that observed for  $\text{Ru}_3(\text{CO})_8(\text{dppm})_2$  [7], in which the dppm ligands are  $\mu_2\text{-}\eta^2$  coordinated, the same coordination mode can be assumed for **3**. Accordingly, the  $^{31}\text{P}\{^1\text{H}\}$  NMR spectrum of **3** shows two signals for two types of phosphorus atoms (Table 1); both signals appear as broad doublets due to the coupling with the second P atom of the dcpm ligands, the couplings between the phosphorus atoms of the different dcpm ligands across the ruthenium skeleton being too small to be observed.

The molecular structure of **3** is confirmed by a single-crystal X-ray structure analysis; the molecule is shown in Fig. 3; important bond lengths and angles are given in Table 4.

Table 2  
Selected bond lengths (Å), bond angles (°) and torsion angles (°) for **1**<sup>a</sup>

Bond lengths			
Ru(1)–Ru(3)	2.8384(7)	Ru(3)–C(109)	1.902(7)
Ru(2)–Ru(3)	2.8378(7)	Ru(3)–C(110)	1.925(8)
Ru(1)–Ru(2)	2.8596(8)	O(1)–C(101)	1.162(10)
Ru(2)–P(1)	2.3462(17)	O(2)–C(102)	1.133(10)
Ru(3)–P(2)	2.3384(15)	O(3)–C(103)	1.148(10)
Ru(1)–C(101)	1.1931(9)	O(4)–C(104)	1.121(9)
Ru(1)–C(102)	1.899(9)	O(5)–C(105)	1.139(9)
Ru(1)–C(103)	1.927(9)	O(6)–C(106)	1.153(9)
Ru(1)–C(104)	1.955(10)	O(7)–C(107)	1.154(9)
Ru(2)–C(105)	1.918(8)	O(8)–C(108)	1.135(8)
Ru(2)–C(106)	1.901(9)	O(9)–C(109)	1.145(8)
Ru(2)–C(107)	1.939(8)	O(10)–C(110)	1.148(9)
Ru(3)–C(108)	1.936(8)		
Bond angles			
Ru(3)–Ru(1)–Ru(2)	59.738(17)	C(105)–Ru(2)–P(1)	93.3(2)
Ru(3)–Ru(2)–Ru(1)	59.760(18)	C(106)–Ru(2)–P(1)	103.1(2)
P(1)–Ru(2)–Ru(1)	152.41(5)	C(107)–Ru(2)–P(1)	89.5(2)
P(1)–Ru(2)–Ru(3)	94.00(4)	C(108)–Ru(3)–P(2)	92.83(19)
P(2)–Ru(3)–Ru(2)	93.03(4)	C(109)–Ru(3)–P(2)	106.8(2)
P(2)–Ru(3)–Ru(1)	60.503(18)	C(110)–Ru(3)–P(2)	85.47(18)
Torsion angles			
P(1)–Ru(2)–Ru(3)–P(2)	11.39(6)		
P(1)–Ru(2)–Ru(3)–Ru(1)	–170.98(5)		
Ru(2)–Ru(1)–Ru(2)–P(2)	5.32(10)		

<sup>a</sup> Details for one of the four independent molecules found per asymmetric unit.

Table 3  
Selected bond lengths (Å), bond angles (°) and torsion angles (°) for **2**

<i>Bond lengths</i>			
Ru(1)–Ru(3)	2.8422(4)	Ru(3)–C(109)	1.932(3)
Ru(2)–Ru(3)	2.8494(4)	Ru(3)–C(110)	1.955(3)
Ru(1)–Ru(2)	2.8684(4)	O(1)–C(101)	1.143(3)
Ru(1)–P(1)	2.3303(7)	O(2)–C(102)	1.138(4)
Ru(2)–P(2)	2.3267(7)	O(3)–C(103)	1.145(3)
Ru(1)–C(101)	1.936(3)	O(4)–C(104)	1.153(3)
Ru(1)–C(102)	1.903(3)	O(5)–C(105)	1.132(4)
Ru(1)–C(103)	1.940(3)	O(6)–C(106)	1.141(3)
Ru(2)–C(104)	1.927(3)	O(7)–C(107)	1.132(4)
Ru(2)–C(105)	1.912(4)	O(8)–C(108)	1.141(4)
Ru(3)–C(106)	1.947(3)	O(9)–C(109)	1.134(3)
Ru(3)–C(107)	1.927(3)	O(10)–C(110)	1.136(3)
Ru(3)–C(108)	1.943(3)		
<i>Bond angles</i>			
Ru(1)–Ru(2)–Ru(3)	60.526(10)	C(101)–Ru(1)–P(1)	90.80(8)
Ru(3)–Ru(1)–Ru(2)	59.861(10)	C(102)–Ru(1)–P(1)	100.83(8)
P(1)–Ru(1)–Ru(3)	153.50(2)	C(103)–Ru(1)–P(1)	92.79(8)
P(1)–Ru(1)–Ru(2)	99.31(2)	C(104)–Ru(2)–P(2)	95.67(8)
P(2)–Ru(2)–Ru(3)	155.87(2)	C(105)–Ru(2)–P(2)	99.52(9)
P(2)–Ru(2)–Ru(1)	100.31(2)	C(106)–Ru(2)–P(2)	91.14(8)
<i>Torsion angles</i>			
P(1)–Ru(1)–Ru(2)–P(2)	31.94(3)		
P(1)–Ru(1)–Ru(2)–Ru(3)	–165.45(2)		
Ru(3)–Ru(1)–Ru(2)–P(2)	17.55(4)		

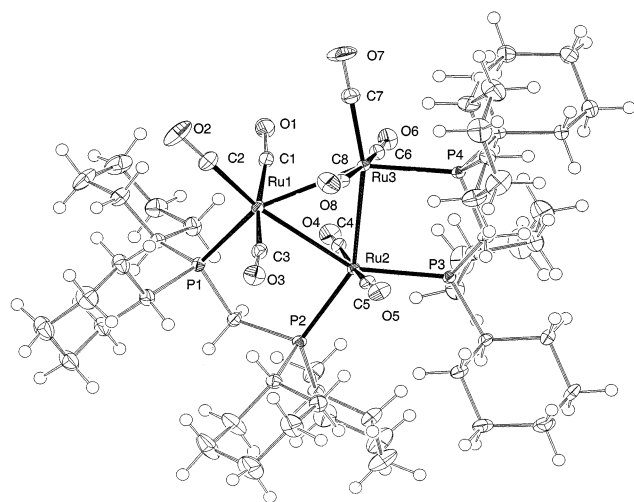


Fig. 3. ORTEP representation of **3**.

The triruthenium core of **3** consists of an asymmetric  $\text{Ru}_3$  triangle where the three metal–metal bonds (2.8357(6), 2.8718(6), 2.8572(5) Å) are slightly longer than those of the  $\text{Ru}_3(\text{CO})_8(\text{dppm})_2$  analogue (2.8268(2), 2.833(2), 2.858(2) Å) [15]. The diphosphine ligands lie in equatorial positions, the phosphorus atoms being slightly out of the metal plane (torsion angles: P(1)–Ru(1)–Ru(2)–P(2)  $-16.88(4)^\circ$ , P(3)–Ru(2)–Ru(3)–P(4)  $-14.60(4)^\circ$ ; distances of the phosphorus atoms from the  $\text{Ru}_3$ -plane: P(1)  $-0.4979(13)$ ,

P(2) 0.1880(12), P(3)  $-0.2448(12)$ , P(4) 0.3512(13) Å). The bulkiness of the  $\text{PCy}_2$  groups causes a larger twist effect for one ligand but a smaller twist effect for the other ligand, as compared to those in the  $\text{PPh}_2$  analogue  $\text{Ru}_3(\text{CO})_8(\text{dppm})_2$  (distances of P-atoms from  $\text{Ru}_3$ -plane: P(1)  $-0.332(5)$ , P(2) 0.303(5), P(3)  $-0.596$ , P(4) 0.285 Å) [15].

In contrast to **3**, which contains the two diphosphine ligands in the classical  $\mu_2$ - $\eta^2$  coordination mode, also observed for  $\text{Ru}_3(\text{CO})_8(\text{dppm})_2$  [15], complex **4** presents a completely different structure with an unprecedented arrangement of the two diphosphine ligands: one F-dppe ligand is  $\mu_2$ - $\eta^2$ -coordinated to two different ruthenium atoms, while the other one is  $\mu_1$ - $\eta^2$ -coordinated to the third ruthenium atom.

The unusual structure of **4** is confirmed by the single-crystal X-ray structure analysis. The molecule is depicted in Fig. 4 and important bond lengths and angles are given in Table 5. The  $\text{Ru}_3$  core can be described as an unsymmetrical triangle, the three metal–metal bonds being Ru(1)–Ru(2) 2.8801(5) Å, Ru(2)–Ru(3) 2.8786(6) Å, Ru(1)–Ru(3) 2.9027(5) Å. The  $\mu_2$ - $\eta^2$  F-dppe ligand is coordinated to Ru(2) and Ru(3) (Ru(2)–P(3) 2.3277(13) Å, Ru(3)–P(4) 2.3122(12) Å) in an equatorial position and the twist effect is larger (distances of the phosphorus atoms from the  $\text{Ru}_3$  plane in **4**: P(1)  $-0.3704(15)$  Å, P(2)  $-0.3976(14)$  Å, P(3) 0.6357(15) Å, P(4)  $-0.3618(14)$  Å) than that in the mono-substituted complex **2**. The second F-dppe ligand coordinates to

Table 4  
Selected bond lengths (Å), bond angles (°) and torsion angles (°) of **3**

<i>Bond lengths</i>			
Ru(1)–Ru(3)	2.8357(6)	Ru(3)–C(6)	1.931(5)
Ru(2)–Ru(3)	2.8572(5)	Ru(3)–C(7)	1.881(5)
Ru(1)–Ru(2)	2.8718(6)	Ru(3)–C(8)	1.932(5)
Ru(1)–P(1)	2.3373(11)	O(1)–C(1)	1.152(6)
Ru(2)–P(2)	2.3688(11)	O(2)–C(2)	1.149(7)
Ru(2)–P(3)	2.3673(12)	O(3)–C(3)	1.145(6)
Ru(2)–P(2)	2.3384(11)	O(4)–C(4)	1.156(6)
Ru(1)–C(1)	1.932(5)	O(5)–C(5)	1.151(6)
Ru(1)–C(2)	1.884(5)	O(6)–C(6)	1.144(6)
Ru(1)–C(3)	1.927(5)	O(7)–C(7)	1.150(6)
Ru(2)–C(4)	1.916(5)	O(8)–C(8)	1.150(6)
Ru(2)–C(5)	1.918(5)		
<i>Bond angles</i>			
Ru(3)–Ru(2)–Ru(1)	59.335(14)	C(2)–Ru(1)–P(1)	101.03(15)
Ru(3)–Ru(1)–Ru(2)	60.077(14)	C(3)–Ru(1)–P(1)	90.17(13)
P(1)–Ru(1)–Ru(3)	151.59(3)	C(4)–Ru(2)–P(2)	87.41(14)
P(1)–Ru(1)–Ru(2)	94.02(3)	C(5)–Ru(2)–P(2)	98.41(13)
P(3)–Ru(2)–Ru(3)	92.35(3)	C(4)–Ru(2)–P(3)	95.00(14)
P(2)–Ru(2)–Ru(3)	150.62(3)	C(5)–Ru(2)–P(3)	86.87(14)
P(3)–Ru(2)–Ru(1)	151.13(3)	C(7)–Ru(3)–P(4)	101.89(15)
P(2)–Ru(2)–Ru(1)	91.60(3)	C(6)–Ru(3)–P(4)	88.61(14)
C(1)–Ru(1)–P(1)	97.63(14)	C(8)–Ru(3)–P(4)	87.41(14)
<i>Torsion angles</i>			
P(1)–Ru(1)–Ru(2)–P(3)	155.30(7)	P(1)–Ru(1)–Ru(3)–Ru(2)	–26.60(6)
P(1)–Ru(1)–Ru(2)–Ru(2)	–16.88(4)	P(3)–Ru(2)–Ru(3)–P(4)	–14.60(4)
Ru(3)–Ru(1)–Ru(2)–P(3)	–12.37(6)	P(2)–Ru(2)–Ru(3)–P(4)	162.03(6)
P(1)–Ru(1)–Ru(2)–Ru(3)	167.67(3)	P(3)–Ru(2)–Ru(3)–Ru(1)	174.06(3)
P(1)–Ru(1)–Ru(3)–P(4)	–45.93(10)	P(2)–Ru(2)–Ru(3)–Ru(1)	–9.31(6)
Ru(2)–Ru(1)–Ru(3)–P(4)	–19.33(7)		

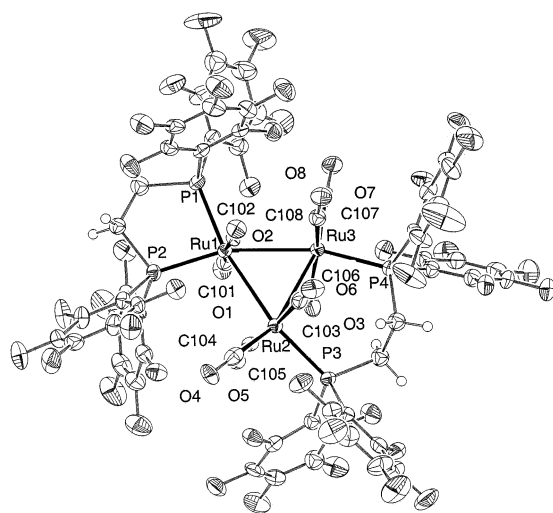


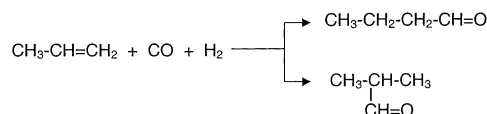
Fig. 4. ORTEP representation of **4**.

Ru(1) in a  $\mu_1\text{-}\eta^2$  fashion, also occupying the equatorial positions of Ru(1), the ruthenium–phosphorus distances are slightly shorter than those in the  $\mu_2\text{-}\eta^2$ -coordinated ligand (Ru(1)–P(1) 2.2891(13) Å, Ru(1)–P(2) 2.3046(12) Å).

In the  $^{31}\text{P}\{^1\text{H}\}$  NMR spectrum, **4** gives rise to two doublets of pseudo-triplets which can be interpreted in

terms of an AA'BB' system. Because of the larger deshielding effect of a five-membered ring with respect to the six-membered ring [16,17], the signal at  $\delta = 35.6$  ppm is assigned to P(1) and P(2), while the signal at  $\delta = 16.5$  ppm is attributed to P(3) and P(4).

The new diphosphine derivatives of  $\text{Ru}_3(\text{CO})_{12}$  have been studied as homogeneous catalysts for the hydroformylation of ethylene and propylene. The reactions were carried out in dimethylformamide (dmf) at 80 °C; apart from a small amount of decomposition, the clusters could be recovered unchanged after the catalytic reaction and reused for further catalytic runs. All clusters **1–4** are active; the results are given in Table 6.



In order to compare the substitution effects on the catalytic activities and selectivities, we also tested  $\text{Ru}_3(\text{CO})_{12}$  and  $\text{Ru}_3(\text{CO})_{10}(\text{dppe})$  under the same conditions. Like  $\text{Ru}_3(\text{CO})_{10}(\text{dppe})$ , the mono-substituted cyclohexyl analogue **1** is more active than  $\text{Ru}_3(\text{CO})_{12}$ , but shows a lower *n/i* selectivity in the case of propylene. The fluorine-containing mono-substituted cluster **2** is

Table 5  
Selected bond lengths (Å), bond angles (°) and torsion angles (°) of **4**

<i>Bond lengths</i>			
Ru(1)–Ru(3)	2.9027(5)	Ru(3)–C(106)	1.924(6)
Ru(2)–Ru(3)	2.8786(6)	Ru(3)–C(107)	1.931(5)
Ru(1)–Ru(2)	2.8801(5)	Ru(3)–C(108)	1.897(6)
Ru(1)–P(1)	2.2891(13)	O(1)–C(101)	1.166(6)
Ru(1)–P(2)	2.3046(12)	O(2)–C(102)	1.150(6)
Ru(2)–P(3)	2.3277(13)	O(3)–C(103)	1.177(6)
Ru(3)–P(4)	2.3122(12)	O(4)–C(104)	1.151(7)
Ru(1)–C(101)	1.930(6)	O(5)–C(105)	1.156(6)
Ru(1)–C(102)	1.951(6)	O(6)–C(106)	1.157(6)
Ru(2)–C(103)	1.909(6)	O(7)–C(107)	1.159(6)
Ru(2)–C(104)	1.913(6)	O(8)–C(108)	1.154(6)
Ru(2)–C(105)	1.930(6)		
<i>Bond angles</i>			
Ru(3)–Ru(1)–Ru(2)	60.538(12)	C(101)–Ru(1)–P(1)	93.73(16)
Ru(2)–Ru(1)–Ru(3)	59.706(13)	C(102)–Ru(1)–P(1)	89.25(15)
P(1)–Ru(1)–Ru(2)	166.25(4)	C(101)–Ru(1)–P(2)	88.26(14)
P(2)–Ru(1)–Ru(2)	105.42(3)	C(102)–Ru(1)–P(2)	99.17(15)
P(1)–Ru(1)–Ru(3)	109.86(3)	C(103)–Ru(2)–P(3)	88.93(15)
P(2)–Ru(1)–Ru(3)	162.38(4)	C(104)–Ru(2)–P(3)	101.07(16)
P(3)–Ru(2)–Ru(3)	102.09(4)	C(105)–Ru(2)–P(3)	95.53(15)
P(3)–Ru(2)–Ru(1)	157.00(4)	C(106)–Ru(3)–P(4)	94.13(14)
P(4)–Ru(3)–Ru(2)	100.44(4)	C(107)–Ru(3)–P(4)	89.49(13)
P(4)–Ru(3)–Ru(1)	158.44(4)	C(108)–Ru(3)–P(4)	99.08(16)
<i>Torsion angles</i>			
P(1)–Ru(1)–Ru(2)–P(3)	–87.27(18)	P(1)–Ru(1)–Ru(2)–Ru(3)	–42.92(15)
P(2)–Ru(1)–Ru(2)–P(3)	125.34(10)	P(2)–Ru(1)–Ru(2)–Ru(3)	169.69(4)
P(1)–Ru(1)–Ru(3)–P(4)	144.89(10)	P(2)–Ru(2)–Ru(3)–Ru(1)	163.78(4)
P(2)–Ru(1)–Ru(3)–P(4)	–59.94(16)	Ru(1)–Ru(2)–Ru(3)–P(4)	170.84(4)
P(3)–Ru(2)–Ru(3)–P(4)	–25.37(5)		

Table 6  
Catalytic activity of **1–4** and of Ru<sub>3</sub>(CO)<sub>12</sub> and Ru<sub>3</sub>(CO)<sub>10</sub>(dppe) for the hydroformylation<sup>a</sup> of ethylene and propylene

Catalyst <sup>b</sup>	Ethylene pressure (bar)	Propylene pressure (bar)	Turnover number <sup>c</sup>	Selectivity <sup>d</sup>
<b>1</b>	10	–	274	–
	–	9	130	71/29
<b>2</b>	10	–	429	–
	–	9	145	57/41
<b>3</b>	10	–	127	–
	–	9	72	83/17
<b>4</b>	10	–	143	–
	–	9	130	67/33
Ru <sub>3</sub> (CO) <sub>12</sub>	10	–	157	–
	–	9	63	85/5
Ru <sub>3</sub> (CO) <sub>10</sub> (dppe)	10	–	289	–
	–	9	128	63/37

<sup>a</sup> Conditions: 10 ml dmf, 10 bar CO, 10 bar H<sub>2</sub>, 80 °C, 24 h.

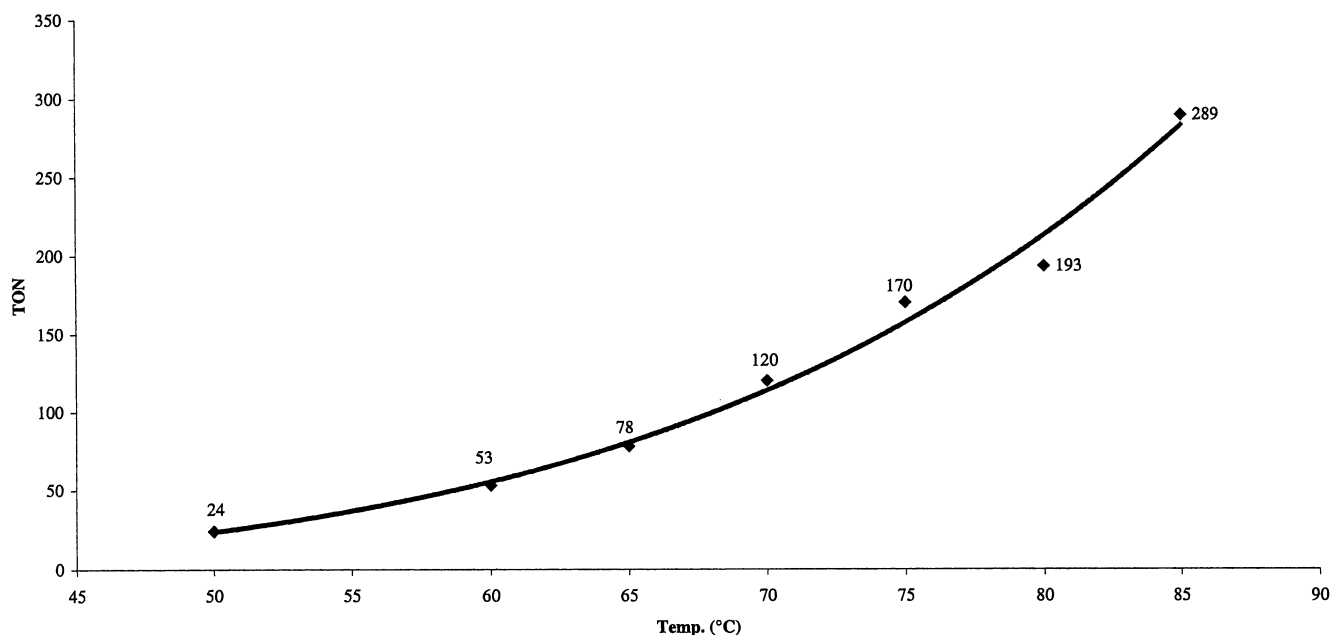
<sup>b</sup> 0.01 mmol.

<sup>c</sup> mol product/mol catalyst.

<sup>d</sup> *n*-Propionaldehyde/*i*-propionaldehyde (%).

more active than **1**, but less selective. The di-substituted clusters **3** and **4** are less active but more selective than the mono-substituted clusters **1** and **2**. The highest turnover number (TON) in the hydroformylation of ethylene is observed with **2**: 429 cycles within 24 h as compared to 157 for Ru<sub>3</sub>(CO)<sub>12</sub> (at 80 °C). For the

most active catalyst **2**, the temperature dependence of the catalytic activity was studied over a temperature range between 50 and 80 °C for 6 h; the results are shown in Fig. 5. The TON–*T* curve exhibits a flat exponential increase of the catalyst reactivity with temperature.



Solvent: dmf (10ml); Pressure: 30 bar ( $H_2/C_2H_4/CO = 10/10/10$ ); Catalyst: 0.01 mmol of **2**; Time: 6h

Fig. 5. Temperature influence over the reactivity of **2**. Solvent, dmf (10 ml); pressure, 30 bar ( $H_2/C_2H_4/CO = 10/10/10$ ); catalyst, 0.01 mmol of **2**; time, 6 h.

### 3. Experimental

All reactions were carried out under an atmosphere of nitrogen using standard Schlenk techniques. Solvents were dried and distilled prior to use as described in the literature [18].  $Ru_3(CO)_{12}$  was prepared from  $RuCl_3 \cdot nH_2O$  and CO according to the literature method [19],  $Ru_3(CO)_{10}(dppe)$  was synthesised as described in [5]; the commercial diphosphines dcpm and F-dppe were used without further purification. The high purity gases  $H_2$ , ethylene, propylene, CO were used as received.  $^1H$ ,  $^{19}F$ ,  $^{31}P$ , and  $^{31}P\{^1H\}$  NMR spectra were recorded on VARIAN Gemini 2000 and BRUKER AMX-400 instruments. The  $^1H$  NMR shifts were referenced to  $CDCl_3$  (internal),  $^{19}F$  and  $^{31}P$  shifts were referenced to external samples ( $PhCF_3$  and 85%  $H_3PO_4$ , respectively). FT-IR spectra were recorded with a Perkin–Elmer 1720X. Elemental analyses were performed by the micro-analytical laboratories of the ETH Zürich and the Université de Genève (Switzerland). The catalytic reactions were studied by means of a gas chromatograph DANI 86.10 equipped with a column CHROMPACK (WCOT fused silica 25 m  $\times$  0.32 mm coating CP-WAS 52 CB), using toluene as the external reference for the quantitative analysis.

#### 3.1. Synthesis of $Ru_3(CO)_{10}(dcpm)$ (**1**) and $Ru_3(CO)_8(dcpm)_2$ (**3**)

A solution of  $Ru_3(CO)_{12}$  (100 mg, 0.15 mmol) in thf

(30 ml) was treated with dcpm [67 mg, 0.15 mmol (for **1** as major product); 201 mg, 0.45 mmol (for **3** as major product)] and refluxed under vigorous stirring. The solution colour changed from orange to red. The reaction was monitored by FT-IR and stopped when the characteristic  $Ru_3(CO)_{12}$  absorption at  $\nu = 2061\text{ cm}^{-1}$  had disappeared; this was the case after 75 min of reflux. Then the solvent was removed under vacuum. The resulting dark-red residue was dissolved in a minimum amount (ca. 5 ml) of  $CH_2Cl_2$ . Preparative thin-layer chromatography of this solution (silica gel 60 GF<sub>254</sub>, Merck) using cyclohexane/ $CH_2Cl_2$  (5:1) as eluent gave unreacted  $Ru_3(CO)_{12}$  (3%) as the first yellow band. The products were extracted from the second red band (**1**) and from the third red band (**3**) with  $CH_2Cl_2$  and recrystallised from dichloromethane. Yields: 42% (**1**); 47% (**3**). Anal. Found: C, 42.15; H, 4.69. Calc. for  $C_{35}H_{46}O_{10}P_2Ru_3$  (**1**): C, 42.38; H, 4.67%. Anal. Found: C, 52.07; H, 7.01. Calc. for  $C_{58}H_{92}O_8P_4Ru_3$  (**3**): C, 51.82; H, 6.89%.

*Alternative preparation of 1:* Sodium diphenylketyl was prepared by reacting benzophenone (91 mg, 0.5 mmol) in dry thf (20 ml) with metallic Na (ca. 200mg) [14]; then a solution of  $Ru_3(CO)_{12}$  (100 mg, 0.15 mmol) in thf (30 ml) was treated with dcpm (67 mg, 0.15 mmol) and heated at 40 °C. Then five drops of the sodium diphenylketyl solution were added and the stirring of the solution at 40 °C was continued until the characteristic  $Ru_3(CO)_{12}$  absorption at  $\nu = 2061\text{ cm}^{-1}$  had disappeared; this was the case after 10 min. Then

the solvent was removed under vacuum. The resulting dark-red residue was dissolved in a minimum amount (ca. 5 ml) of  $\text{CH}_2\text{Cl}_2$ . The product (**1**) was isolated by preparative thin-layer chromatography of this solution (silica gel 60 GF<sub>254</sub>, Merck), using cyclohexane– $\text{CH}_2\text{Cl}_2$  (5:1) as eluent, from the main red band. Crystallisation from dichloromethane gave **1** in 77% yield.

### 3.2. Synthesis of $\text{Ru}_3(\text{CO})_{10}(\text{F-dppe})$ (**2**) and $\text{Ru}_3(\text{CO})_8(\text{F-dppe})_2$ (**4**)

A solution of  $\text{Ru}_3(\text{CO})_{12}$  (150 mg, 0.24 mmol) in thf (30 ml) was treated with F-dppe (179 mg, 0.24 mmol (for **2** as major product); 537 mg, 0.72 mmol (for **4** as major product)) and refluxed under vigorous stirring. The solution colour changed from orange to red. The reaction was monitored by FT-IR and stopped when the characteristic  $\text{Ru}_3(\text{CO})_{12}$  absorption at  $\nu = 2061 \text{ cm}^{-1}$  disappeared; this was the case after 16 h of reflux. Then the solvent was removed under vacuum. The resulting orange–red residue was dissolved in a minimum amount (ca. 5 ml) of  $\text{CH}_2\text{Cl}_2$ . Preparative thin-layer chromatography of this solution (silica gel 60 GF<sub>254</sub>, Merck) using cyclohexane/ $\text{CH}_2\text{Cl}_2$  (1:1) as eluent, gave unreacted  $\text{Ru}_3(\text{CO})_{12}$  (1%) as the first yellow band. The products were extracted from the second red band (**2**) and from the third red band (**4**) with  $\text{CH}_2\text{Cl}_2$  and recrystallised from dichloromethane for **2** and dichloromethane/methanol (9:1) for **4**. Yields: (**2**) 36%; (**4**) 32%. Anal. Found: C, 32.28; H 0.16. Calc. for  $\text{C}_{36}\text{H}_4\text{O}_{10}\text{F}_{20}\text{P}_2\text{Ru}_3$  (**2**): C, 32.23; H, 0.3%. Anal. Found: C, 35.07; H, 0.58. Calc. for  $\text{C}_{60}\text{H}_8\text{F}_{40}\text{P}_4\text{Ru}_3$  (**4**): C, 35.26; H, 0.39%.

*Alternative preparation of 3:* Sodium diphenylketyl was prepared as described below [14], then a solution of  $\text{Ru}_3(\text{CO})_{12}$  (100 mg, 0.15 mmol) in thf (30 ml) was treated with F-dppe (224 mg, 0.30 mmol) and heated at 40 °C. Then five drops of the sodium diphenylketyl solution were added and the stirring of the solution at 40 °C was continued until the characteristic  $\text{Ru}_3(\text{CO})_{12}$  absorption at  $\nu = 2061 \text{ cm}^{-1}$  had disappeared; this was the case after 25 min. The solution was filtered (unreacted F-dppe) and then, the solvent was removed under vacuum. The resulting dark-red residue was dissolved in a minimum amount (ca. 5 ml) of  $\text{CH}_2\text{Cl}_2$ . The product (**3**) was isolated by preparative thin-layer chromatography of this solution (silica gel 60 GF<sub>254</sub>, Merck), using cyclohexane/ $\text{CH}_2\text{Cl}_2$  (4:1) as eluent, from the main red band. Crystallisation from dichloromethane gave **3** in 79% yield.

### 3.3. Crystallography

Suitable crystals of **1–3** were grown from  $\text{CH}_2\text{Cl}_2$  and **4** from  $\text{CH}_2\text{Cl}_2/\text{MeOH}$  (9:1). For **1**, intensity data were collected at 153 K on a Stoe image plate diffrac-

tion system (Stoe & Cie, 1995) using Mo K $\alpha$  graphite monochromated radiation; the imaging plate distance was 90 mm,  $\Phi$  oscillation scans 0–180°, step  $\Delta\Phi = 0.5^\circ$ ,  $2\theta$  range 2.54–45.0°,  $d_{\text{max}} - d_{\text{min}} = 16.00 - 0.93 \text{ \AA}$ . For **2**, imaging plate distance was 90 mm,  $\Phi$  oscillation scans 0–184°, step  $\Delta\Phi = 0.5^\circ$ ,  $2\theta$  range 2.54–45.0°,  $d_{\text{max}} - d_{\text{min}} = 16.00 - 0.93 \text{ \AA}$ . For **3** and **4**, data collection was performed at 153 K using Mo K $\alpha$  radiation ( $\lambda = 0.71073 \text{ \AA}$ ), 200 exposures (3 min per exposure), imaging plate distance 70 mm,  $\Phi$  oscillation scans 0–200°, step  $\Delta\Phi = 1^\circ$ ,  $d_{\text{max}} - d_{\text{min}} = 12.445 - 0.81 \text{ \AA}$ . All structures were solved by direct methods using the programme SHELXS-97 [20]. The refinement and all further calculations were carried out using SHELXL-97 [21]. The H atoms were included in calculated positions

Table 7  
Crystal data and structure refinement parameters for **1** and **2**

	<b>1</b>	<b>2</b>
Empirical formula	$\text{C}_{35}\text{H}_{42}\text{O}_{10}\text{P}_2\text{Ru}_3$	$\text{C}_{36}\text{H}_4\text{F}_{20}\text{O}_{10}\text{P}_2\text{Ru}_3 \cdot 1/2(\text{CH}_2\text{Cl}_2)$
Formula weight	987.84	1384.00
Crystal system	orthorhombic	triclinic
Crystal shape	block	rod
Crystal colour	orange	red
Space group	$Pca2_1$	$P\bar{1}$
Unit cell dimensions		
<i>a</i> (Å)	27.1737(12)	13.1110(10)
<i>b</i> (Å)	11.0849(6)	17.7259(12)
<i>c</i> (Å)	52.721(3)	20.8427(15)
$\alpha$ (°)	90	71.947(8)
$\beta$ (°)	90	79.706(9)
$\gamma$ (°)	90	71.491(8)
<i>V</i> (Å <sup>3</sup> )	15880.5(14)	4349.9(5)
<i>Z</i>	16	4
<i>D</i> <sub>calc</sub> (g cm <sup>-3</sup> )	1.653	2.113
Absorption coefficient (mm <sup>-1</sup> )	1.259	1.305
<i>F</i> (000)	7904	2652
Crystal size (mm)	0.45 × 0.45 × 0.25	0.35 × 0.20 × 0.10
Angle range	2.29 < $\theta$ < 25.77	2.02 < $\theta$ < 25.91
Index ranges	–23 ≤ <i>h</i> ≤ 28, –10 ≤ <i>k</i> ≤ 11, –56 ≤ <i>l</i> ≤ 55	–16 ≤ <i>h</i> ≤ 16, –21 ≤ <i>k</i> ≤ 21, –25 ≤ <i>l</i> ≤ 24
Reflections measured	21 638	31 507
Reflections observed	14 561	11 602
Independent reflections	15 546	15 720
<i>R</i> <sub>int</sub>	0.0309	0.023
Radiation used	Mo K $\alpha$	Mo K $\alpha$
<i>R</i> <sub>1</sub> [ <i>I</i> > 2 $\sigma$ ( <i>I</i> )]	0.0243, 0.0270	0.0222, 0.0381
<i>R</i> <sub>1</sub> (all data) <sup>a</sup>		
<i>wR</i> <sub>2</sub> [ <i>I</i> > 2 $\sigma$ ( <i>I</i> )]	0.0579, 0.0590	0.0442, 0.0466
<i>wR</i> <sub>2</sub> (all data) <sup>b</sup>		
Goodness-of-fit on <i>F</i> <sup>2</sup> <sup>c</sup>	0.973	0.820

<sup>a</sup>  $R_1 = \Sigma(|F_o| - |F_c|) / \Sigma|F_o|$ .

<sup>b</sup>  $wR_2 = [\Sigma w(F_o^2 - F_c^2)^2 / \Sigma(F_o^2)^4]^{1/2}$ .

<sup>c</sup>  $S = [\Sigma w(F_o^2 - F_c^2)^2 / (n - p)]^{1/2}$  (*n* = number of reflections, *p* = number of parameters), calc.  $w = 1 / [\sigma^2(F_o^2)1(0.0431P)^2 + 0.0000P]$  where  $P = (F_o^2 + 2F_c^2) / 3$ .

and treated as riding atoms using SHELXL-97 default parameters. In **1**, there are four independent molecules per asymmetric unit and the structure was refined as a racemic twin with BASF finally equal to 0.237(17). For **2**, two independent molecules of **2** and one molecule of CH<sub>2</sub>Cl<sub>2</sub> were found per asymmetric unit. The non-H atoms were refined anisotropically, using weighted full-matrix least-squares on  $F^2$ . Compound **3** crystallises with two molecules of CH<sub>2</sub>Cl<sub>2</sub> per asymmetric unit; one of the two solvent molecules is strongly disordered and occupies two different sites in space, each being occupied by 50%. Atoms having occupancies less than 0.5 are refined isotropically. In **4**, there is one molecule per asymmetric unit (Flack parameter  $x = -0.04(2)$ ).

Table 8  
Crystal data and structure refinement parameters for **3** and **4**

	<b>3</b>	<b>4</b>
Empirical formula	C <sub>58</sub> H <sub>92</sub> O <sub>8</sub> Ru <sub>3</sub> ·2CH <sub>2</sub> Cl <sub>2</sub>	C <sub>60</sub> H <sub>8</sub> F <sub>40</sub> O <sub>8</sub> P <sub>4</sub> Ru <sub>3</sub> ·CH <sub>2</sub> Cl <sub>2</sub> ·0.25CH <sub>3</sub> OH
Formula weight	1514.26	2136.69
Crystal system	triclinic	orthorhombic
Crystal shape	plate	plate
Crystal colour	yellow	yellow
Space group	$P\bar{1}$	$Pc2_1b$
Unit cell dimensions		
$a$ (Å)	12.2135(11)	13.1721(7)
$b$ (Å)	12.8211(11)	22.3255(11)
$c$ (Å)	23.344(2)	25.9838(13)
$\alpha$ (°)	82.374	90
$\beta$ (°)	80.439	90
$\gamma$ (°)	74.675	90
$V$ (Å <sup>3</sup> )	3461.3(5)	7641.2(7)
$Z$	2	4
$D_{\text{calc}}$ (g cm <sup>-3</sup> )	1.453	1.857
Absorption coefficient (mm <sup>-1</sup> )	0.941	0.888
$F(000)$	1560	4122
Crystal size (mm)	0.60 × 0.50 × 0.25	0.50 × 0.1 × 0.08
Angle range	1.65 < $\theta$ < 26.05	1.65 < $\theta$ < 26.05
Index ranges	-14 ≤ $h$ ≤ 14, -15 ≤ $k$ ≤ 15, -28 ≤ $l$ ≤ 28	-16 ≤ $h$ ≤ 16, -27 ≤ $k$ ≤ 27, -31 ≤ $l$ ≤ 31
Reflections measured	27093	58321
Reflections observed	10874	10569
Independent reflections	12439	14795
$R_{\text{int}}$	0.0440	0.0676
Radiation used	Mo K $\alpha$	Mo K $\alpha$
$R_1$ [ $I > 2\sigma(I)$ ], $R_1$ (all data) <sup>a</sup>	0.0463, 0.0524	0.0323, 0.0536
$wR_2$ [ $I > 2\sigma(I)$ ], $wR_2$ (all data) <sup>b</sup>	0.1358, 0.1406	0.0550, 0.0588
Goodness-of-fit on $F^2$ <sup>c</sup>	1.041	0.800

$$^a R_1 = \sum(|F_o| - |F_c|) / \sum|F_o|$$

$$^b wR_2 = [\sum w(F_o^2 - F_c^2)^2 / \sum(F_o^2)^4]^{1/2}$$

$$^c S = [\sum w(F_o^2 - F_c^2)^2 / (n - p)]^{1/2} \quad (n = \text{number of reflections, } p = \text{number of parameters), calc. } w = 1 / [\sigma^2(F_o^2)1(0.0431P)^2 + 0.0000P] \text{ where } P = (F_o^2 + 2F_c^2)/3.$$

Strongly disordered solvent molecules of dichloromethane and methanol were found; it was not possible to define the atom positions correctly. The program SQUEEZE [22] was used to solve this problem and a solvent accessible area was calculated with 373 electrons in the unit cell corresponding to approximately four molecules of dichloromethane and one molecule of methanol (372 electrons). The figures were drawn with PLATON-99 [22]. Crystal data for compounds **1–4** are given in Tables 7 and 8.

### 3.4. Catalytic reactions

All catalytic reactions were carried out in a glass-line stainless-steel autoclave (100 ml of capacity). A solution of dmf (10 ml) containing 0.01 mmol of catalyst was placed in the autoclave and degassed by bubbling nitrogen through the solution. The autoclave was purged three times with the olefin, then pressurised with the gas mixture and heated in an oil bath to the required temperature ( $\pm 1$  °C) with continuous stirring. After the indicated reaction time, the autoclave was rapidly cooled with ice, the pressure was released, the products and the solvent were separated from the catalyst by vacuum distillation. The remaining solid was studied by IR and NMR spectroscopy to ensure catalyst recovery. The solution obtained was studied by gas chromatography using toluene (0.025%) as the external reference to quantify the products.

## 4. Supplementary material

Crystallographic data for the structural analysis have been deposited with the Cambridge Crystallographic Data Centre, CCDC Nos. 158020, 158021, 158022 and 158023 for compounds **1–4**, respectively. Copies of this information may be obtained free of charge from The Director, CCDC, 12 Union Road, Cambridge, CB2 1EZ, UK (fax: +44-1223-3360333; e-mail: deposit@ccdc.cam.ac.uk or www: http://www.ccdc.cam.ac.uk).

## Acknowledgements

The authors are grateful to the Swiss National Science Foundation for financial support and to the Johnson Matthey Technology Centre for a generous loan of ruthenium chloride hydrate.

## References

- [1] A.J. Deeming, in: E.W. Abel, F.G.A. Stone, G. Wilkinson (Eds.), *Comprehensive Organometallic Chemistry II*, Pergamon, Oxford, 1995, pp. 711–721.

- [2] A.W. Coleman, D.F. Jones, P.H. Dixneuf, C. Brisson, J.-J. Bonnet, G. Lavigne, *Inorg. Chem.* 23 (1984) 952.
- [3] G. Lavigne, J.-J. Bonnet, *Inorg. Chem.* 20 (1981) 2713.
- [4] H.A. Mirza, J.-J. Vittal, R.J. Puddephatt, *Inorg. Chem.* 32 (1993) 1327.
- [5] M.I. Bruce, T.W. Hambley, B.K. Nicholson, M.R. Snow, *J. Organomet. Chem.* 235 (1982) 83.
- [6] B. Fontal, M. Reyes, T. Suárez, F. Bellandi, J.C. Diaz, *J. Mol. Catal.* 149 (1999) 75.
- [7] B. Fontal, M. Reyes, T. Suárez, F. Bellandi, J.C. Diaz, *J. Mol. Catal.* 149 (1999) 87.
- [8] C. Bergounhou, J.J. Bonnet, P. Fompeyrine, G. Lavigne, N. Logun, F. Mansilla, *Organometallics* 5 (1985) 60.
- [9] C. Bergounhou, J.J. Bonnet, P. Fompeyrine, G. Commenges, *J. Mol. Catal.* 48 (1988) 285.
- [10] H.C. Böttcher, G. Rheinwald, H. Stoeckli-Evans, G. Süß-Fink, *J. Organomet. Chem.* 520 (1996) 163.
- [11] H.C. Böttcher, H. Thönnessen, P.G. Jones, R. Schmutzler, *J. Organomet. Chem.* 520 (1996) 15.
- [12] G. Süß-Fink, I. Godefroy, V. Ferrand, A. Neels, H. Stoeckli-Evans, *J. Chem. Soc., Dalton Trans.* (1998) 515.
- [13] G. Süß-Fink, I. Godefroy, V. Ferrand, A. Neels, H. Stoeckli-Evans, S. Kahlal, J.-Y. Saillard, M.-T. Garland, *J. Organomet. Chem.* 579 (1999) 285.
- [14] M.I. Bruce, J.G. Matison, B.K. Nicholson, *J. Organomet. Chem.* 247 (1983) 321.
- [15] G. Lavigne, N. Lugan, J.J. Bonnet, *Acta Crystallogr., Sect. B* 38 (1982) 1911.
- [16] M.R. Churchill, R.A. Lashewycz, J.R. Shapley, S.I. Richter, *Inorg. Chem.* 19 (1980) 1277.
- [17] S.O. Grim, W.L. Briggs, R.C. Barth, C.A. Tolman, J.P. Jesson, *Inorg. Chem.* 13 (1974) 1095.
- [18] D.D. Perrin, W.L.F. Armarego, *Purification of Laboratory Chemicals*, 3rd ed., Pergamon, Oxford, 1989.
- [19] M.I. Bruce, C. Jensen, N.L. Jones, *Inorg. Synth.* 26 (1989) 259.
- [20] G.M. Sheldrick, *SHELXS-97: Program for Crystal Structure Determination*, *Acta Crystallogr., Sect. A* 46 (1990) 467.
- [21] G.M. Sheldrick, *SHELXL-97: Program for Crystal Structure Refinement*, University of Göttingen, Göttingen, Germany, 1999.
- [22] A.L. Spek, *Acta Crystallogr., Sect. A* 46 (1990) C34.